Volume 2 | Number 48 | 28 December 2014 | Pages 10221–10478

Journal of Materials Chemistry C

Materials for optical, magnetic and electronic devices

www.rsc.org/MaterialsC

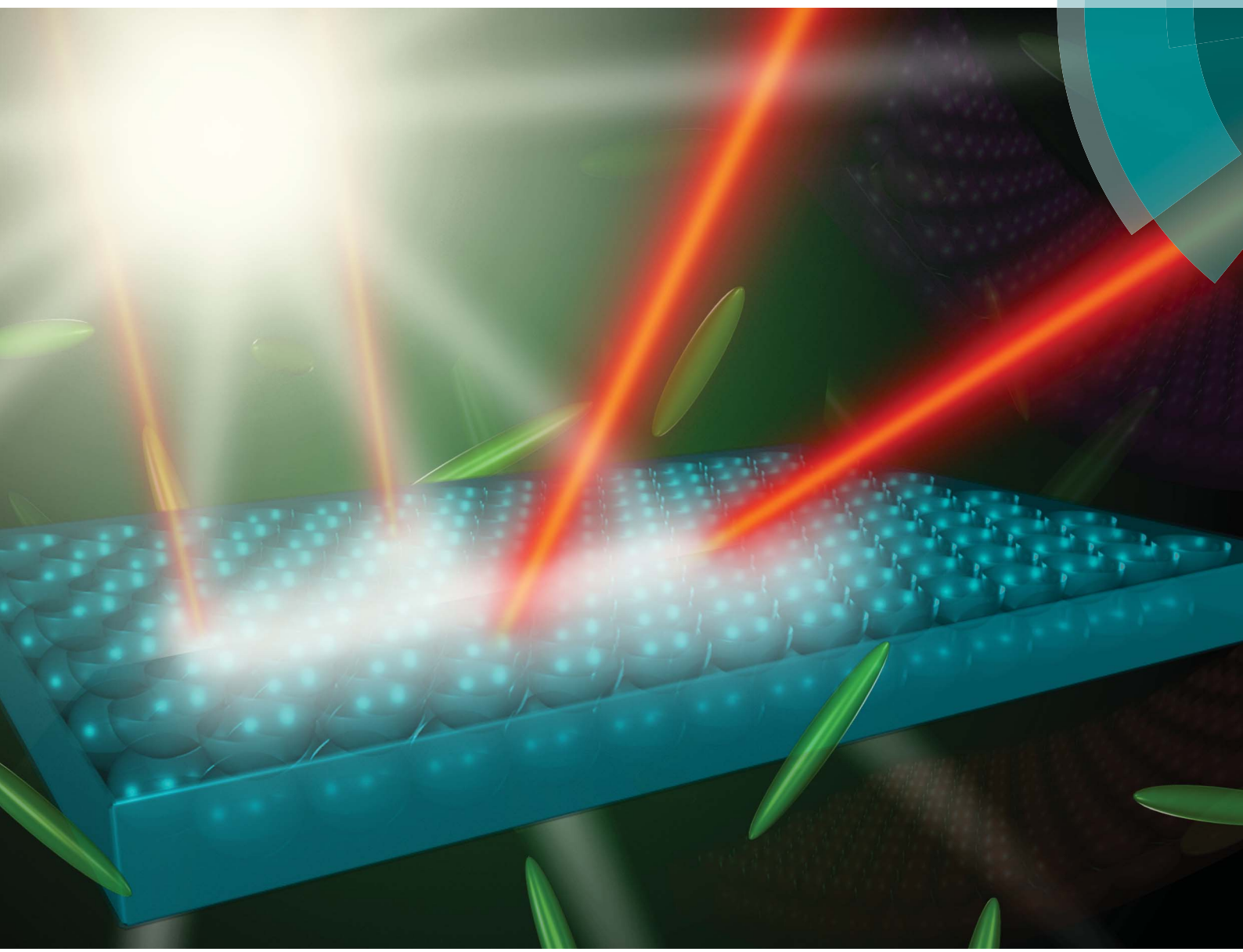

ISSN 2050-7526

ROYAL SOCIETY OF CHEMISTRY

COMMUNICATION

Yanlei Yu *et al.*

Dual-responsive inverse opal films based on a crosslinked liquid crystal polymer containing azobenzene

Journal of Materials Chemistry C

COMMUNICATION

View Article Online
View Journal | View Issue

Cite this: J. Mater. Chem. C, 2014, 2, 10262

Received 19th August 2014
Accepted 4th October 2014

DOI: 10.1039/c4tc01825g

www.rsc.org/MaterialsC

Dual-responsive inverse opal films based on a crosslinked liquid crystal polymer containing azobenzene†

Jianqiang Zhao, Yuyun Liu and Yanlei Yu*

Novel photo and thermal dual-responsive inverse opal films were fabricated based on a crosslinked liquid crystal polymer (CLCP) containing azobenzene. Accompanying the deformation of the CLCP, switchable behavior on the reflection spectra of the inverse opal film was induced by light or temperature. We found that the optical properties were drastically decreased by thermal or photoinduced phase transitions of the CLCP. It was also found that the extent of decrease in the heat-induced inverse opal film is much more than in the one induced by light.

Introduction

Photonic crystal structures have generated a great amount of interest due to their unique properties in controlling the propagation of light.[1] Recently, the capability for tuning the band structure through external stimuli has been investigated for many potential applications;[2–5] this can be controlled through the lattice constants[6] and the refractive indices of the dielectrics.[7,8] Due to their unique properties, liquid crystal (LC) materials have been employed to obtain tunable photonic crystals in response to a single stimulus, such as light, temperature, and electric field.[9–12]

Sato and coworkers[7] reported a switchable photonic crystal that exhibited a drastic change in optical properties by taking advantage of the photoinduced phase transition of LC, which was comprised of SiO_2 inverse opal infiltrated by nematic LC (5CB) and photochromic LC azo dyes. However, 5CB and azo dyes are free in the holes of SiO_2 inverse opal, and the matrix of SiO_2 is a hard material, which are drawbacks for photonic crystals in practical applications.

Crosslinked liquid crystal polymers (CLCPs) are unique materials that possess the properties of both LCs and elastomers.[13] The coupling of LC order and rubber elasticity results in an anisotropic polymer network that can respond to various external stimuli, such as temperature,[14–17] light,[18–20] magnetic field,[21] and electricity,[22–24] followed by a significant and reversible change in their shapes.

Keller and coworkers created a microarray of a main-chain CLCP using the replica molding technique and found that the pillar showed ultralarge and reversible contraction during thermal phase transition.[25] Zentel and coworkers prepared monodisperse and monodomainic, micrometer-sized CLCP beads by the use of a microfluidic setup. The beads exhibited a strong and rapid shape change of about 70% in length by heat.[26]

By incorporating azobenzene moieties into the CLCPs, large deformations such as contraction,[27,28] bending[29–33] and helical motion[34] have also been realized by the photochemical reactions of these azobenzene chromophores. van Oosten *et al.* succeeded in the preparation of an artifical microcilia array using CLCPs by inkjet printing technology.[35] The artifical microcilia array underwent bending under irradiation of UV and visible light, respectively. In our previous work, we fabricated a microarrayed CLCP film using polydimethylsiloxane-soft-template-based secondary replication.[36] The microarrayed film showed reversible switch of superhydrophobic adhesion by alternating irradiation of UV and visible light.

Due to the abovementioned stimuli-responsive deformations, CLCPs have recently been considered to be a good candidate for future photonic crystals. Our group prepared a 2D photonic crystal with the azobenzene-containing CLCP by using the replica molding technique. We found that the reflection spectra of the microarray showed switchable behavior upon the irradiation of UV light.[37] However, CLCPs are seldom used as inverse opal materials for tunable photonic crystals. Compared with 2D photonic crystals, inverse opal materials have been demonstrated to exhibit excellent photonic crystal properties, such as the

Department of Materials Science & State Key Laboratory of Molecular Engineering of Polymers, Fudan University, 220 Handan Road, Shanghai 200433, China. E-mail: ylyu@fudan.edu.cn

† Electronic supplementary information (ESI) available: Synthesis and characterization of monomers and CLCPs, the crosslinking density influence on double-responsive properties, the amount of energy for stimulation, and deformation of the azobenzene-containing CLCP films. This material is available free of charge *via* the Internet at http://pubs.rsc.org. See DOI: 10.1039/c4tc01825g

presence of optical stop bands, tunable color changes, and especially high reflection intensity. Li and coworkers first made the inverse opal material using CLCP together with a nematic LC (5CB) that was introduced directly into the photonic crystal.[38] When the temperature was close to the nematic-to-isotropic transition (T_{NI}), the lattice structure changed, which led to the continuous blue shift of the Bragg peak. Also, the intensity of the reflection spectra decreased significantly. However, because 5CB molecules were not linked directly to the CLCP by covalent bonds, they moved freely in the inverse opal material; thus the reversibility of the blue shift was not good. Later, they prepared a new type of electrothermally driven photonic crystal film based on highly crosslinked CLCP without 5CB.[39] When a 30 V electric field was applied on the CLCP inverse opal films to make them close to their T_{NI}, where the LC moieties become isotropic, the films started to contract along the nematic director axis. During this process, the holes in the films changed from round to ellipse, which led to a shift of the reflection peaks. However, this is a comparatively complex process because of the preparation of the electrodriven setup. In this paper, light/thermal dual-responsive inverse opal films were first fabricated from an azobenzene CLCP by infiltrating the ordered assembly of silica spheres with a precursor capable of solidification, and then removing the SiO_2 template. Here, we used an LC crosslinker instead of the reported isotropic crosslinker, which gives the inverse opal films good repeatability and different responsiveness from the reported CLCP inverse opal films. It was found that the reflection spectra of the inverse opal films showed switchable behavior when irradiated with UV light or heated. This phenomenon is ascribed to the change in the order of the periodic structure of the holes.

Experimental

Materials

All solvents and chemicals were of reagent quality and used without further purification unless specified. THF was purified by distillation. 6-chloro-1-hexanol and 3-bromo-1-propanol were purchased from Alfa. 4-methoxyphenol and 4-hydroxybenzonitrile were purchased from Aladdin. Photoinitiator Irgarcure 784 was purchased from Ciba. The monodispersed nanosilica spheres were purchased from Nanjing Dongjian Biological Technology Co. The monomers A6Bz1, A6BCN, C3A, and DA6AB were synthesized according to the literature.[40] The chemical structures of the monomers are shown in Scheme 1a. The synthesis routes and ^{1}H NMR spectra are shown in ESI (Scheme S1 and Fig. S1†).

Preparation of azo inverse opal films

The close-packed, face-centered cubic (FCC) photonic crystal film with a thickness of several micrometers was prepared by the two-substrate vertical deposition method in anhydrous ethanol with monodispersed silica spheres (350 nm diameter).[41] Scheme 1 illustrates the preparation of the inverse opal film based on the CLCP. The inverse opal film was prepared by copolymerization as follows: first, a certain amount of the mixture of A6Bz1, A6BCN, C3A and DA6AB with the molar ratio of 6 : 2 : 1 : 1 containing 2 mol% of a photoinitiator was dissolved in CH_2Cl_2. Then, the melt of the mixture was injected into the sandwich of the SiO_2 opal film between the glass and PMMA plates. During this procedure, the reactant mixture was infiltrated into the voids of the opal film, then cooled down slowly (0.2 °C min^{-1}) to polymerization temperatures, which were set at 2 °C below the clearing points of the mixture (nematic phase). Polymerization was performed at >540 nm with a high-pressure Hg lamp through glass filters (Toshiba, Y-52 and IRA-25S) for 2 h. The polymer was then immersed in 1% HF solution for several hours to completely remove the silica colloids. After that, we obtained the CLCP-based, free-standing inverse opal film.

Measurements

The thermodynamic properties of the LC mixture and the CLCP inverse opal film were characterized with differential scanning calorimetry (DSC, TA, Q2000) at heating and cooling rates of 3 °C min^{-1} for the mixture and 10 °C min^{-1} for the film. Three scans were applied to check the reproducibility. The mesomorphic properties were studied using a polarizing optical microscope (POM, Leica DM4000M) equipped with a Mettler hot stage (Linkam, T95-PE and LNP95). The morphology of the inverse opal film was observed by SEM (Zeiss, Ultra 55). The reflection spectra of the inverse opal film were measured using a multichannel photo detector connected to a Y-type optical fiber. The light source was a deuterium-halogen lamp (Micropack, DH 2000), and the range of the wavelength of the detector (Ideaoptics, PG 2000) was from 400 to 1000 nm. A UV-LED irradiator (OMRON, ZUV-C10H, = 365 nm) and a vis-LED irradiator (CCS Inc, HLV-24GR-3W, = 530 nm) were used to induce photoisomerization of the azobenzene moieties.

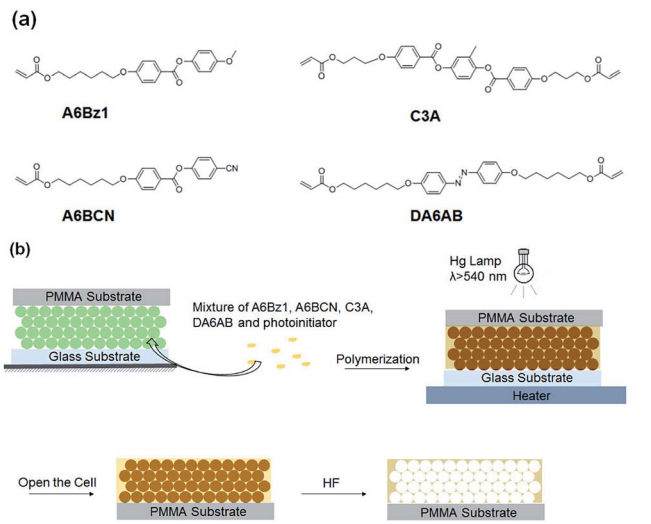

Scheme 1 (a) The chemical structures of the LC monomers A6Bz1, A6BCN, C3A and DA6AB. (b) The fabrication process of the CLCP inverse opal film.

Results and discussion

Topography and mesomorphic properties

The topographical character of the inverse opal films was investigated by SEM. Fig. 1 shows SEM images of the opal structure composed of SiO_2 spheres with a diameter of 350 nm and the CLCP-based inverse opal film. It should be noted that after etching the silica template by using 1 wt% HF aqueous solution, the resulting CLCP-based inverse opal film was directly used for SEM imaging, and no more extra treatments were performed for the SEM samples. Fig. 1a and c show the top and side SEM images of the thin colloidal crystal. It is clear that the opal film has a closely packed hexagonal structure with long-range regulation. The images of the inverse opal film in Fig. 1b and d derived from the FCC opal structure confirm that the opal structure has been successfully replicated. Polydispersity of the hole diameters is possible because the surface of the silica template is not smooth. However, the locally amplified SEM image of the inverse opal film in Fig. 1d demonstrates that the diameter of the inside holes in the inverse opal film is monodispersed. Therefore, polydispersity of the hole diameters only occurs on the surface of the inverse opal film.

The thermodynamic properties and the phase transitions of the monomer and mixture were investigated by POM and DSC. The results of the phase transition are listed in Table S1.† A6Bz1, C3A and the mixture all show a LC phase over a wide temperature range. The distinct schlieren textures of A6Bz1, C3A and DA6AB ascribed to the nematic phase were observed with POM (Fig. S2†).

The results of DSC measurement on the obtained inverse opal films are shown in Fig. S3.† The inverse opal film exhibited a glass transition around 27 °C, which allows the inverse opal films to undergo deformations at room temperature. Above T_g, an exothermal peak exists on the curve between 70 °C and 90 °C assigned to the phase transition from the nematic to isotropic phase.

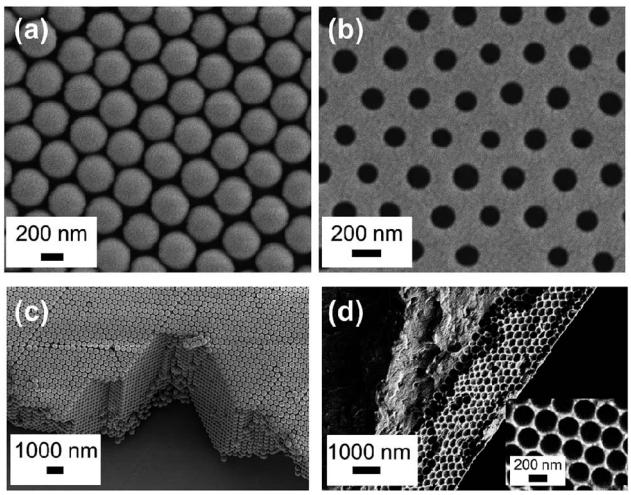

Fig. 1 SEM surface images of (a) the SiO_2 opal film and (b) the CLCP inverse opal film, and SEM cross section images of (c) the SiO_2 opal film and (d) the CLCP inverse opal film. The inset is the locally amplified image. Thickness of the inverse opal film is about 17 μm.

Repeatable photoresponse behavior

The repeatable photoresponse behavior of the CLCP-based inverse opal film was investigated by the Y-type optical fiber to observe the change in UV-vis reflection spectra. As shown in Fig. 2, a large amount of light is reflected at 677 nm wavelength and cannot pass through the CLCP inverse opal film in the initial state. When the film was exposed to UV light (365 nm, 50 mW cm^{-2}), the intensity of the reflection peak at 677 nm sharply declined. During this process, the maximum intensity of the reflection peak changed from 90% to 20%. In other words, a maximum intensity contrast of more than 77% was realized. When we used visible light (20 mW cm^{-2}) instead of UV light, the observed intensity of the reflection peak partially recovered. With the extension of exposure time, the intensity of the reflection peak gradually increased until it reached the maximum value of 70% under the irradiation of visible light. Though there was a little difference with the original value prior to UV light irradiation, the results still demonstrate the repeatability of the reflection peak intensity. More details on the dynamics of the reflection peak during UV and visible light irradiation are shown in Fig. S4.†

This phenomenon in the CLCP inverse opal film is caused by the photoinduced deformation of the CLCP. Under UV irradiation, the azobenzene moieties change from *trans* rodlike shape to *cis* bent shape, causing contraction of the film surface. However, because the CLCP inverse opal film is a polydomain LC film, the direction of contraction is not uniform, which disturbs the regular, periodic porous structure.[42] Meanwhile, upon visible light irradiation, the azobenzene groups transform to their original states, which in turn results in recovery of the periodic structure. In other words, the periodic holes in the inverse opal film undergo a change from regular to irregular in response to UV light. This has been verified by SEM images of the inverse opal film before and after UV light irradiation (Fig. 3).

Moreover, a polydomain, azobenzene-containing, free standing film that has the same composition as the inverse opal film was also prepared. When irradiated with UV light, the

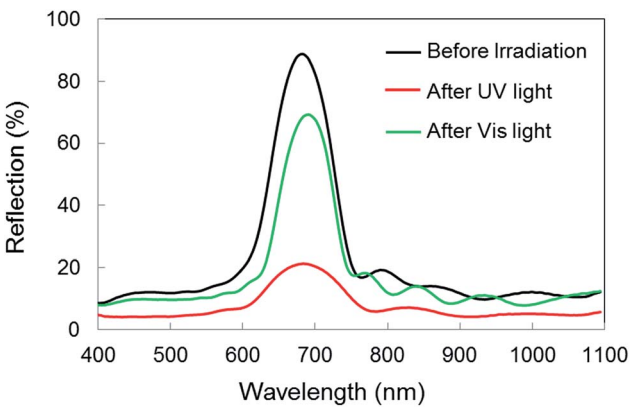

Fig. 2 Reflection spectra of the azobenzene CLCP inverse opal film under UV light irradiation (365 nm, 50 mW cm^{-2}, 5 min) and subsequent visible light irradiation (530 nm, 20 mW cm^{-2}, 15 min).

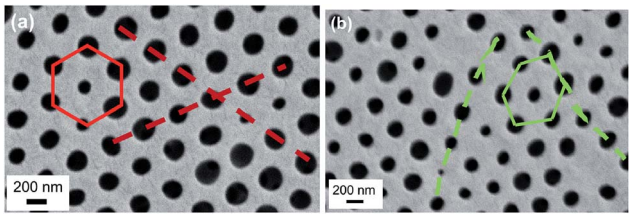

Fig. 3 SEM images of the inverse opal film (a) before and (b) after UV light irradiation. The red regular hexagon and straight lines represent the arrangement of the holes before UV light irradiation; the green hexagon and lines represent the arrangement of the holes after irradiation with UV light. After UV light irradiation, the shape of the hexagon becomes irregular, and the straight lines have become curves.

square-shaped polydomain film randomly bent toward the light source due to its unhomogeneous contraction (Fig. S5†). The bending deformation is ascribed to the *trans–cis* photoisomerization of the azobenzene units and the subsequent photochemical changes in size and alignment order of the azobenzene moieties in the CLCP film driven by UV light, which were observed by POM and UV-vis absorption spectra. The POM images of the polydomain CLCP film are shown in Fig. S6.† We can see that there is almost no difference between the two images, because the CLCP film is a polydomain film, and the photochemical change only occurs in the surface region of the film.[32] As shown in Fig. S7,† the absorption spectrum in the initial state exhibited a distinct band, which corresponds to the π–π* transitions of the azobenzene chromophores. When the film was irradiated with UV light (365 nm, 20 mW cm^{-2}), the photoisomerization process was monitored by absorption spectroscopy. The absorption band of the π–π* transitions gradually decreased with a concomitant increase in the band around 460 nm (*n*–π* transition), indicating the occurrence of *trans–cis* isomerization of the azobenzene moieties in the CLCP film (Fig. S7a†). The reversible absorption change can be achieved by visible light irradiation at 530 nm (Fig. S7b†).

The repeatable use of the inverse opal films is significant for industrial applications. Fig. 4 shows five cycles of the alternate irradiation of UV and visible light, which illustrates the stability of the materials. The change in the maximum intensity of the reflection peak could be repeatedly induced by alternate irradiation of UV and visible light. The intensity of the reflection peaks is a little lower than the initial reflection peak when the cycle number is 3, 5, 7 and 9, because the order of the changed periodic structure cannot be returned to its initial periodic structure order.

Temperature-induced, repeatable response behavior

Fig. 5 shows the reflection spectra for the inverse opal film as a function of temperature. The intensity of the reflection peak at 677 nm sharply declined with the increase of the temperature. When the film was heated to 90 °C, the reflection peak at 677 nm almost disappeared, which is different from that of above-mentioned photoresponsive behavior. In other words, complete switching was realized during the heating process. This is because the LC moieties become isotropic, and the film starts to contract in all directions when the temperature is close to the nematic-to-isotropic transition. The degree of contraction of the heated inverse opal film is larger than that induced by UV light, which only irradiates the surface region of the film; thus, there is a greater thermally induced disturbance of the periodic porous structure order, contributing to the complete switching. We also checked the thermoinduced contraction of the azobenzene-containing, free-standing film. Thermoinduced contraction is different from photoinduced contraction of the azobenzene-containing CLCP film. When the temperature is increased, the entire square-shaped polydomain film randomly contracted. Thus, the CLCP film contracted in the macroscopic scale, which was different from that in photoinduced deformation (Fig. S9†). Since the shape and/or size of the CLCP films can recover to their original states by cooling due to the repeatable transition of the LC order, the intensity of the reflection peak gradually increased and reached the maximum value of 70% when the temperature decreased. Though there was a little difference from the original value, the result still demonstrates the repeatability of the intensity of the reflection peak.

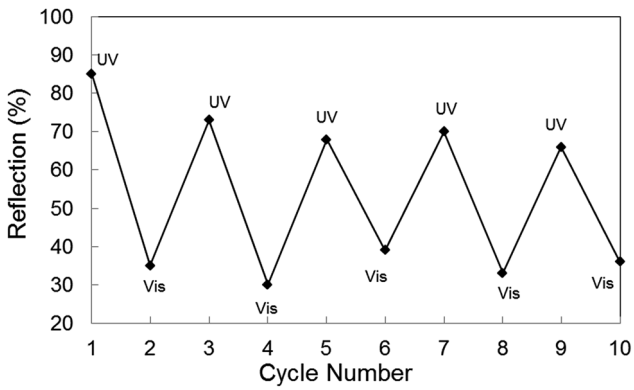

Fig. 4 The maximum intensity of the reflection peak of the inverse opal film under alternating irradiation with UV and visible light at different times.

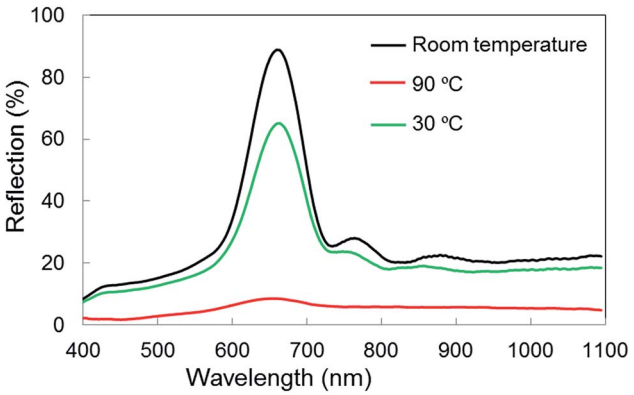

Fig. 5 Reflection spectra of the inverse opal film as a function of temperature.

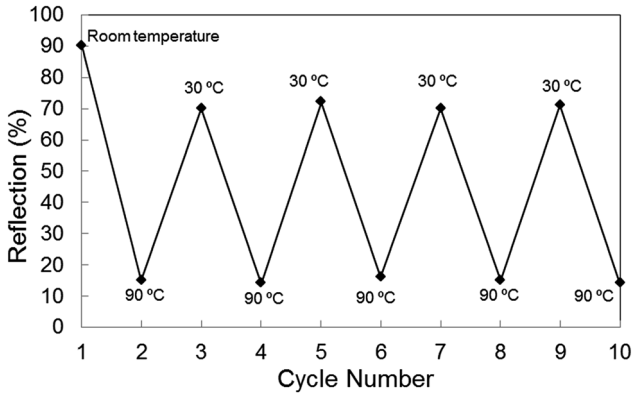

Fig. 6 Five low-high temperature cycles of the reflection peak maximum intensity of the inverse opal film.

Finally, the changes in maximum intensity of the reflection peak of the CLCP inverse opal at 677 nm are shown in Fig. 6. Though the maximum intensity of reflection peaks at cycle numbers 3, 5, 7 and 9 is a little lower than the initial value, the results suggest that the inverse opal film has good repeatability of the reflection peak.

Here, we estimated the amount of light and heat energy that gave rise to responsive behavior. As shown in Fig. S8,† the CLCP inverse opal film can be heated to 90 °C in 3 s (about 0.9 J), while the amount of energy is about 1.06 J for the light irradiation process (365 nm, 50 mW cm^{-2}, 5 min), which is larger than that of the heating process. More detailed information is described in the ESI.†

We also prepared and studied the dual responsive properties of the inverse opal films with different crosslinking densities by varying the feed concentration of the crosslinker C3A from 0 to 90 mol% in the polymerizable mixture. As shown in Fig. S10 and S11,† the change in the maximum intensity of the reflection spectra becomes smaller with the increased feed concentration of C3A. Moreover, the switching behavior of the inverse opal film without C3A is not repeatable.

Conclusion

A new type of dual-responsive inverse opal was fabricated based on the azobenzene-containing CLCP. The inverse opal film showed switchable behavior on the reflection spectra by alternate irradiation of UV-vis light or temperature, owing to the change in the order of the holes. This change in the periodic structure is ascribed to the contraction of CLCP induced by the photochemical reactions of the azobenzene moieties or the thermal-induced phase transition. It is the first time that azobenzene-containing CLCPs have been used to prepare inverse opal film and achieve repeatable switching behavior on the film's reflection spectra using light, which can be manipulated conveniently and controlled *in situ*. This work presents a critical advance that will broaden the practical applications of azobenzene-containing CLCPs.

Acknowledgements

This work was supported financially from the National Natural Science Foundation of China (nos 51225304, 21134003, 21273048, and 51203023), and Shanghai Natural Science Foundation (no. 12ZR1401600).

Notes and references

1 O. Sato, S. Kubo and Z. Z. Gu, *Acc. Chem. Res.*, 2009, **42**, 1.
2 M. Moritsugu, T. Shirota, S. Kubo, T. Ogata, O. Sato and S. Kurihara, *J. Polym. Sci., Part B: Polym. Phys.*, 2009, **47**, 1981.
3 R. Tatsumi, J. I. Mamiya, M. Kinoshita and A. Shishido, *Sci. Adv. Mater.*, 2014, **6**, 1432.
4 A. Priimagi, C. J. Barrett and A. Shishido, *J. Mater. Chem. C*, 2014, **2**, 7155.
5 H. L. Lei and Y. Zhao, *Polymer*, 1994, **35**, 104.
6 Y. Y. Diao, X. Y. Liu, G. W. Toh, L. Shi and J. Zi, *Adv. Funct. Mater.*, 2013, **23**, 5373.
7 S. Kubo, Z. Z. Gu, K. Takahashi, Y. Ohko, O. Sato and A. Fujishima, *J. Am. Chem. Soc.*, 2002, **124**, 10950.
8 S. Kubo, Z. Z. Gu, K. Takahashi, A. Fujishima, H. Segawa and O. Sato, *J. Am. Chem. Soc.*, 2004, **126**, 8314.
9 C. Fenzl, T. Hirsch and O. S. Wolfbeis, *Angew. Chem., Int. Ed.*, 2014, **53**, 3318.
10 K. R. Phillips, N. Vogel, Y. H. Hu, M. Kolle, C. C. Perry and J. Aizenberg, *Chem. Mater.*, 2014, **26**, 1622.
11 S. L. Li, M. Fu, Y. N. Zhang, J. H. Duan, D. W. He and Y. S. Wang, *J. Mater. Chem. C*, 2013, **1**, 5072.
12 S. C. Padmanabhan, K. Linehan, S. O'Brien, S. Kassim, H. Doyle, I. M. Poyey, M. Schmidt and M. E. Pemble, *J. Mater. Chem. C*, 2014, **2**, 1675.
13 F. T. Cheng, Y. Y. Zhang, R. Y. Yin and Y. L. Yu, *J. Mater. Chem.*, 2010, **20**, 4888.
14 P. G. D. Gennes, *C. R. Hebd. Seances Acad. Sci., Ser. B*, 1975, **280**, 9.
15 R. Stannarius, A. Eremin, K. Harth, M. Morys, A. DeMiglio, C. Ohm and R. Zentel, *Soft Matter*, 2012, **8**, 1858.
16 Z. Q. Pei, Y. Yang, Q. M. Chen, E. M. Terentjev, Y. Wei and Y. Ji, *Nat. Mater.*, 2014, **13**, 36.
17 J. E. Marshall, S. Gallagher, E. M. Terentjev and S. K. Smoukov, *J. Am. Chem. Soc.*, 2014, **136**, 474.
18 T. Ikeda, J. Mamiya and Y. L. Yu, *Angew. Chem., Int. Ed.*, 2007, **46**, 506.
19 H. F. Yu and T. Ikeda, *Adv. Mater.*, 2011, 2149.
20 J. Wei and Y. L. Yu, *Soft Matter*, 2012, **8**, 8050.
21 J. P. Ge, Y. X. Hu and Y. D. Yin, *Angew. Chem., Int. Ed.*, 2007, **46**, 7428.
22 E. P. Chan, J. J. Walish, A. M. Urbas and E. L. Thomas, *Adv. Mater.*, 2013, **25**, 3934.
23 X. Feng, B. D. Yang, Y. M. Liu, Y. Wang, C. Dagdeviren, Z. J. Liu, A. Carlson, J. Y. Li, Y. G. Huang and J. A. Rogers, *Acs Nano*, 2011, **5**, 3326.
24 J. J. Walish, Y. Kang, R. A. Mickiewicz and E. L. Thomas, *Adv. Mater.*, 2009, **21**, 3078.
25 H. Yang, A. Buguin, J. M. Taulemesse, K. Kaneko, S. Mery, A. Bergeret and P. Keller, *J. Am. Chem. Soc.*, 2009, **131**, 15000.

26 C. Ohm, E. K. Fleischmann, I. Kraus, C. Serra and R. Zentel, *Adv. Funct. Mater.*, 2010, **20**, 4314.
27 H. Finkelmann, E. Nishikawa, G. G. Pereira and M. Warner, *Phys. Rev. Lett.*, 2001, **87**, 015501.
28 S. Tsoi, J. Zhou, C. Spillmann, J. Naciri, T. Ikeda and B. Ratna, *Macromol. Chem. Phys.*, 2013, **214**, 734.
29 A. Priimagi, A. Shimamura, M. Kondo, T. Hiraoka, S. Kubo, J. I. Mamiya, M. Kinoshita, T. Ikeda and A. Shishido, *ACS Macro Lett.*, 2012, **1**, 96.
30 Y. Y. Zhang, J. X. Xu, F. T. Cheng, R. Y. Yin, C. C. Yen and Y. L. Yu, *J. Mater. Chem.*, 2010, **20**, 7123.
31 Y. L. Yu, M. Nakano and T. Ikeda, *Nature*, 2003, **425**, 145.
32 Y. L. Yu, M. Nakano, A. Shishido, T. Shiono and T. Ikeda, *Chem. Mater.*, 2004, **16**, 1637.
33 M. Kondo, Y. L. Yu and T. Ikeda, *Angew. Chem., Int. Ed.*, 2006, **45**, 1378.
34 S. Iamsaard, S. J. Asshoff, B. Matt, T. Kudernac, J. J. L. M. Cornelissen, S. P. Fletcher and N. Katsonis, *Nat. Chem.*, 2014, **6**, 229.
35 C. L. van Oosten, C. W. M. Bastiaansen and D. J. Broer, *Nat. Mater.*, 2009, **8**, 677.
36 C. Li, F. T. Cheng, J. A. Lv, Y. Zhao, M. J. Liu, L. Jiang and Y. L. Yu, *Soft Matter*, 2012, **8**, 3730.
37 Z. Yan, X. M. Ji, W. Wu, J. Wei and Y. L. Yu, *Macromol. Rapid Commun.*, 2012, **33**, 1362.
38 G. L. Wu, Y. Jiang, D. Xu, H. Tang, X. Liang and G. T. Li, *Langmuir*, 2011, **27**, 1505.
39 Y. Jiang, D. Xu, X. S. Li, C. X. Lin, W. N. Li, Q. An, C. A. Tao, H. Tang and G. T. Li, *J. Mater. Chem.*, 2012, **22**, 11943.
40 B. Yan, J. He, P. Ayotte and Y. Zhao, *Macromol. Rapid Commun.*, 2011, **32**, 972.
41 X. Chen, Z. M. Chen, N. Fu, G. Lu and B. Yang, *Adv. Mater.*, 2003, **15**, 1413.
42 M. Honda, K. Kataoka, T. Seki and Y. Takeoka, *Langmuir*, 2009, **25**, 8349.